EEET ECOLOGICAL ENGINEERING & ENVIRONMENTAL TECHNOLOGY

Ecological Engineering & Environmental Technology, 2026, 27(3), 209–222
https://doi.org/10.12912/27197050/218153
ISSN 2719–7050, License CC-BY 4.0

Received: 2026.01.20
Accepted: 2026.02.19
Published: 2026.03.01

Validation of satellite-derived data for hydrological soil erosion estimation using the RUSLE model in Google Earth Engine: Comparison with field measurements in the Nekor watershed (Rif, Morocco)

Salma Abrouri[1], Ahmed Mahmoud Ahmed Oubeid[1,2], Basma Naoui[1], Sakina Mehdioui[1*], Mohamed Tayebi[1]

[1] Geosciences and Natural Resources Laboratory, Department of Geology, Faculty of Sciences, Ibn Tofail University, BP 133, Kenitra 14000, Morocco
[2] Geosciences Research Unit, Faculty of Sciences and Techniques, University of Nouakchott, Mauritania
* Corresponding author's e-mail: mehdiouisakina@gmail.com

ABSTRACT

This study evaluates the reliability of satellite-derived datasets for estimating hydrological soil erosion estimation by validating Google Earth Engine (GEE)-based RUSLE outputs against field-measured and conventionally GIS-processed data in the Nekor watershed (northern Morocco) over a 40-year period (1983–2023). The watershed, which supplies the Mohamed Ben Abdelkrim El Khattabi Dam, has experienced accelerated sedimentation due to intensified surface runoff, marl-schist degradation, and declining vegetation cover. Soil erosion was estimated using the RUSLE model within two parallel frameworks: (i) a ground-based GIS approach incorporating locally calibrated field data, and (ii) a multi-source satellite-driven workflow implemented in GEE. Long-term temporal trends were analyzed to assess erosion dynamics and evaluate the effectiveness of soil conservation measures introduced in the early 2000. Results from the field-based GIS approach indicate a 16.5% reduction in mean annual soil loss, decreasing from 47.87 to 39.96 t ha^{-1} yr^{-1} over the study period. Comparable trends were observed in the GEE-derived estimates, which declined from 46.08 to 37.04 t ha^{-1} yr^{-1}. Statistical validation demonstrates very strong agreement between the two approaches, with coefficients of determination (R^2) of 0.99 and 0.98 for the two analyzed periods. Error metrics further confirm the robustness of the satellite-based methodology, with high Nash-Sutcliffe efficiency values (NSE = 0.97 in 2003 and 0.96 in 2023), low root mean square error (RMSE = 12.43 and 18.22 t ha^{-1} yr^{-1}), and low mean absolute error (MAE = 10.00 and 15.61 t ha^{-1} yr^{-1}), accompanied by minimal bias (+2.62 and +3.01), indicating only slight overestimation by GEE. Spatial analysis further reveals high concordance in the identification of critical erosion hotspots, particularly in steep upstream areas characterized by fragile lithology and sparse vegetation cover. The novelty of this study lies in the long-term (four-decade) quantitative validation of GEE-based RUSLE outputs against locally calibrated field and GIS datasets in a Mediterranean mountain watershed, providing rare empirical evidence of the accuracy, consistency, and scalability of cloud-based erosion modeling. Overall, the results demonstrate that satellite-derived datasets processed within GEE offer a robust, scalable, and cost-effective alternative for long-term soil erosion monitoring and watershed management, particularly in data-scarce Mediterranean environments.

Keywords: soil erosion; RUSLE; Google Earth Engine; field validation; remote sensing; Nekor watershed.

INTRODUCTION

Water is a vital yet limited resource in Morocco, where precipitation is highly irregular in both space and time and occurs predominantly in mountainous regions (OSS, 2020). Among the principal threats to soil and water sustainability, water erosion represents one of the most significant natural processes, particularly in mountainous and semi-arid environments. Soil erosion results from the combined

effects of rainfall intensity, topography, soil characteristics, and land-use practices, and is further intensified by increasing anthropogenic pressures (Morgan, 2005; FAO, 2015). This process leads to the detachment, transport, and loss of fertile topsoil under the joint action of precipitation, surface runoff, and land-use change.In Morocco, soil erosion is particularly severe in the Rif region, where fragile lithological formations, steep slopes, and high demographic pressure interact with unsustainable agricultural and land-management practices, leading to accelerated environmental degradation (Niazi et al., 2005; Arrebei et al., 2019). Soil erosion rates in these mountainous areas frequently exceed 2,000 $t \cdot km^{-2} \cdot yr^{-1}$, largely due to the overexploitation of natural resources and the progressive decline of vegetation cover (OSS, 2020). The Nekor watershed, located in the eastern Rif massif within Al Hoceïma Province, illustrates these erosion dynamics. Covering approximately 916 km^2, the basin is characterized by rugged topography, marl-dominated lithology highly susceptible to erosion, and a semi-arid Mediterranean climate marked by short-duration, high-intensity rainfall events (Chalouan et al., 2008; Salhi et al., 2019). These natural conditions promote active water erosion and severe gully formation, which are further exacerbated by deforestation, overgrazing, and the expansion of agricultural activities on steep slopes (Lal, 2001). Nekor drains into the Abdelkrim El Khatabi Dam, commissioned in 1981, which provides drinking water to the city of Al Hoceïma and irrigation water for the Nekor plain. However, the reservoir is increasingly threatened by sedimentation caused by high soil loss rates in the upstream catchment (Benmansour et al., 2020). According to Salhi et al. (2022), the degradation of vegetation cover and the intensification of unsustainable agricultural practices significantly accelerate sediment delivery, threatening the dam's storage capacity and long-term regional water security. In this context, understanding soil erosion dynamics is essential for sustainable watershed management and reservoir protection. The present study aims to analyze the spatiotemporal evolution of soil erosion in the Nekor watershed over a 40-year period (1983–2023), divided into two distinct phases: 1983–2003 and 2004–2023. The objectives are to quantify changes in erosion intensity, identify erosion-prone areas, and delineate priority zones for land-use planning and soil conservation measures. To estimate soil losses contributing to sedimentation in the Abdelkrim El Khatabi Dam, the Revised Universal Soil Loss Equation (RUSLE) was applied. Originally developed by Wischmeier and Smith (1978) and later refined by Renard et al. (1997), RUSLE estimates average annual soil loss (A) as a function of five key factors: rainfall erosivity (R), soil erodibility (K), slope length and steepness (LS), land cover and management (C), and conservation support practices (P). However, despite the widespread application of the RUSLE model in combination with remote sensing (RS) and Geographic Information Systems (GIS), conventional approaches continue to face several limitations. These include constraints related to localized data storage, limited computational capacity, and restricted access to comprehensive and frequently updated geospatial datasets. Moreover, RS-based soil erosion assessments often require substantial manual effort for data acquisition, preprocessing, and data integration, which increases processing time and costs and delays the availability of results. Consequently, evaluating soil erosion risk using traditional GIS-based methods remains time-consuming and resource-intensive (Jodhani et al., 2023). Recent advances in cloud computing have enabled the development of more efficient alternatives. Google Earth Engine (GEE) addresses these limitations by providing a cloud-based geospatial analysis platform that offers direct access to extensive satellite imagery archives, global environmental datasets, and automated processing tools. GEE facilitates the computation of RUSLE factors by enabling continuous access to key inputs such as precipitation data, soil properties, topographic information, and land use/land cover (LULC) datasets, while allowing rapid and repeatable LULC classification. In addition, the platform supports the integration of user-provided datasets, including ground-based measurements, to complement satellite-derived information (Papaiordanidis et al., 2019). The integration of RUSLE within the GEE environment significantly reduces computational constraints, enhances processing efficiency, and enables the generation of consistent spatiotemporal soil erosion estimates, which are essential for dynamic and adaptive soil conservation planning. Although the RUSLE–GEE framework has been successfully applied in various regions worldwide, existing studies have largely focused on spatial erosion patterns, with limited attention given to long-term temporal analysis and model validation using field-measured data (Elnashar et al., 2021; Fentaw et al., 2024). In Morocco, and particularly in the Rif region, such integrated and validated approaches remain scarce. This highlights a clear knowledge

gap in the long-term, multi-decadal assessment of soil erosion using cloud-based RUSLE applications, as well as in the rigorous validation of satellite-derived estimates against field measurements in complex mountainous watersheds. To address this gap, the present study develops and systematically validates an integrated RUSLE–GEE framework to assess the spatiotemporal evolution of soil erosion in the Nekor watershed over a 40-year period (1983–2023). The novelty of this research lies in (i) the multi-decadal reconstruction of erosion trends using harmonized satellite-derived datasets, and (ii) the quantitative validation of GEE-based outputs against ground-measured and conventionally GIS-processed erosion estimates within the same watershed. The central scientific hypothesis of this study is that satellite-derived datasets processed within GEE can reproduce long-term erosion dynamics with a level of accuracy statistically comparable to field-based GIS modelling, even in data-scarce and topographically complex environments. Furthermore, it is hypothesized that integrating multi-source remote sensing data enables the detection of temporal shifts in erosion intensity linked to land cover changes and conservation interventions implemented since the early 2000. Accordingly, the primary purpose of this study is to determine whether GEE-based RUSLE modelling can serve as a reliable and validated approach for long-term soil erosion assessment in Mediterranean mountainous watersheds. Specifically, this research aims to (i) quantify the degree of statistical agreement between satellite-driven and ground-based erosion estimates, (ii) identify spatial patterns of convergence and divergence between these methods, and (iii) provide insights into temporal erosion trends over four decades. By achieving these objectives, the study seeks to fill the existing knowledge gap in multi-decadal, validated satellite-based soil erosion modelling and offer a scientifically robust framework to support watershed monitoring and sediment management strategies.

MATERIAL AND METHODS

Study area

The study focuses on the Nekor watershed, located in the central Rif region, with geographical boundaries between latitudes 34°69' and 35°19' N and longitudes 3°36' and 4°00' W, covering an area of 916 km^2 (Fig. 1).

From a demographic perspective, this region is characterized by a high population density, predominantly composed of sedentary farmers belonging to an aging population (El Abassi, 1997; Okacha, 2020). The area benefits from maritime humidity, which moderates the thermal contrasts typically associated with semi-arid zones. Precipitation is scarce and highly irregular, averaging around 346 mm per year, while the mean annual temperature is approximately 18 °C (Salhi, 2008, El Hammoudani, 2021).

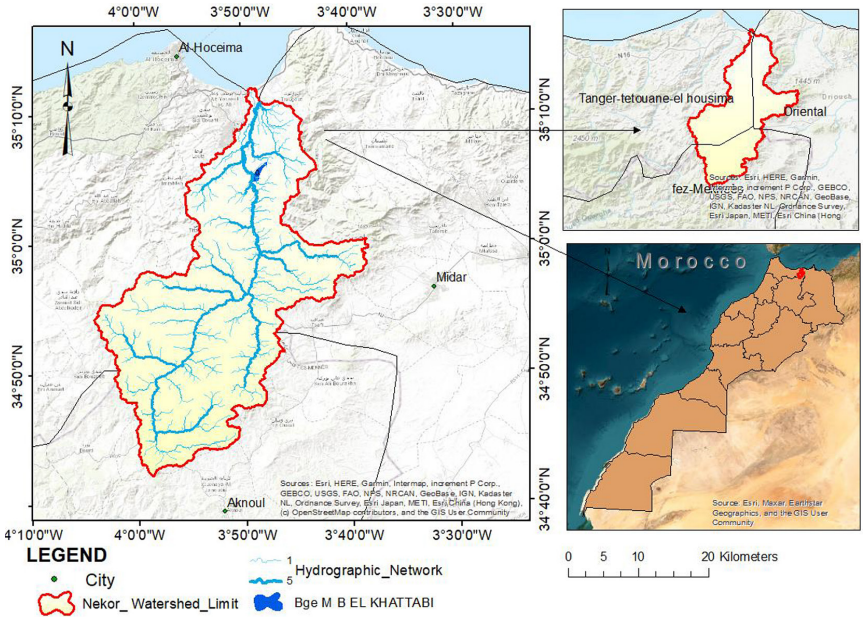

Figure. 1. Nekor watershed's geographic location

The subsurface of the watershed is largely composed of soft lithological units, primarily marls and shales (Laouina, 1995). These rocks are highly friable and prone to rapid disintegration under the action of atmospheric processes. As a result, the soils that develop from them tend to be shallow, underdeveloped, and lack structural cohesion. This intrinsic vulnerability is manifested in a high erodibility value (K-factor in the RUSLE model), suggesting that the soil is easily mobilized by water. From a geological perspective, the region is dominated by fragile shaly and marl-shale formations that are highly prone to erosion. The left bank is mainly composed of shales and limestones, whereas the right bank exhibits a more heterogeneous lithology, including sandstones and limestones. These shallow soils, deficient in organic matter, create conditions that favor gully erosion. Hydrologically, the Watershed is drained by streams with a torrential regime, characterized by irregular but intense floods. The Nekor River is intermittent, while the Rhis-Nekor alluvial aquifer represents a critical water resource, currently threatened by aridity, intensive agricultural practices, and seawater intrusion, despite the presence of the Mohammed Ben Abdelkrim Al Khattabi dam (Iouzzi, 2011). The climate is semi-arid Mediterranean, with an average annual precipitation of approximately 340 mm, mostly occurring in autumn and winter, and temperatures ranging from 7 °C in winter to 28 °C in summer. This climatic context, combined with the watershed topography and soil characteristics, promotes rapid surface runoff and accentuates soil erosion, with notable impacts on the region's hydraulic infrastructure (Niazi et al., 2005).

Methodology

The rate of water-induced soil erosion is primarily governed by four key factors: vegetation cover, soil properties, topography, and climatic conditions (Dwight et Smit, 1957). Land management and soil conservation practices directly influence these factors, thereby contributing to erosion reduction. These variables are incorporated into the RUSLE equation, an empirically based and widely recognized model for estimating the average annual soil loss in a given area (Wischmeier et Smith, 1978). The mathematical formulation of this model is expressed as follows (Fig. 2):

$$E = LS \times C \times R \times K \times P \quad (1)$$

where: E represents the mean annual soil loss, expressed in tons per hectare per year ($t.ha^{-1}.yr^{-1}$); R denotes the rainfall erosivity factor, measured in $MJ.mm.ha^{-1}.h^{-1}.yr^{-1}$; K refers to the intrinsic susceptibility of the soil to erosion ($t.h.N^{-1}.ha^{-1}$); LS is the dimensionless topographic factor combining slope length and steepness; C expresses the influence of vegetation cover and land management practices on soil erosion, dimensionless; P accounts for the effect of soil conservation measures, also dimensionless.

R factor – rainfall erosivity

The R factor quantifies rainfall intensity in terms of its capacity to detach soil particles through mechanical action under conditions of non-concentrated surface runoff (Fig. 3c, 3d). It is expressed in $MJ.mm.ha^{-1}.h^{-1}.yr^{-1}$and refers to

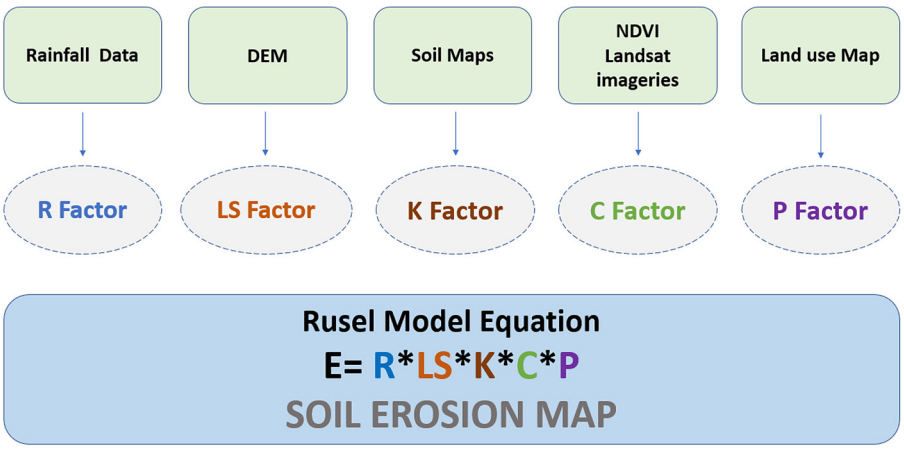

Figure. 2. RUSLE model methodology

a standardized surface without vegetation and with a 9% slope. For Morocco's climatic context, Arnoldus (1977, 1980) proposed a calculation method based on Fournier's rainfall index, expressed as:

$$R = 0.264 \times (i{=}1\sum 12 Pi2/P)1{,}5 \quad (2)$$

where: Pi represents the mean monthly precipitation (mm) and P the mean annual rainfall (mm).

This formula was applied to generate an iso-erosivity map suitable for areas with a semi-arid Mediterranean climate. The rainfall data used in this study were obtained from the observation network of the Loukoss Hydraulic Basin Agency (ABHL). The conversion from U.S. customary units to the metric system was performed using a correction coefficient of 1.735, as recommended by Maaliou et al. (2014). The spatial distribution of the R factor is generated using the Inverse Distance Weighting (IDW) interpolation technique, which assigns weights to observations based on their distance from the target location. This approach is preferred for modeling the spatial pattern of rainfall erosivity, as it minimizes the influence of distant or anomalous data points (Franke & Nielson, 1980; Setianto, 2013).

Topographic factor (LS)

The LS factor represents the combined influence of slope length and gradient on water erosion processes. It is a dimensionless coefficient that quantifies the topographic contribution to soil loss. Its calculation is based on the equation proposed by Moore and Burch (1986), which incorporates two fundamental components: surface runoff accumulation and slope angle (Fig. 3e). The adopted formula is expressed as:

$$LS = [As/\ 22{,}13]^m \times [\sin\beta/0{,}0896]^n \quad (3)$$

where: As – the upslope contributing area (m²), derived from the Digital Elevation Model (DEM); β – the slope angle in radians; m – 0.4; n = 1.3.

Using a high-resolution DEM allows precise derivation of these parameters, thereby facilitating the identification of areas where topographic characteristics increase susceptibility to erosion, particularly on long or steep slopes.

Soil erodibility factor (K)

The K factor expresses the susceptibility of soils to particle detachment caused either by the impact of raindrops or by the shear stress exerted by surface runoff. It reflects the mechanical resistance of soil materials to erosion under standardized conditions, assuming constant topography, vegetation, and land management practices. In the Oued Nekor watershed, the analysis was conducted using publicly available geological and soil datasets for Morocco, compiled from national mapping systems and the Fertimap database. Soil characterization included the estimation of surface rock fragment cover for each soil unit, based on field transect surveys conducted in accordance with FAO guidelines for soil description (FAO, 2006).The evaluation of the K factor was based on reference values from regional studies (Direction des Eaux et Forêts, 1995; Heusch, 1970; Dumas, 1965), following the classification proposed by Manrique (1988), which is consistent with the system used for North African soils (Fig. 3f). This factor is expressed in standardized metric units as:

$$K=(\text{ton}\cdot\text{h})\ /(\text{N}\cdot\text{ha}) \quad (4)$$

Cover management factor (C)

The C factor represents the influence of vegetation cover and cropping practices on soil erosion. It is defined as the ratio between the soil loss observed under a given land cover type and that measured on bare soil (García-Orenes et al., 2009; García-Orenes et al., 2010). A lower C value indicates greater soil protection. In this study, the C factor was derived from Landsat 5 (2003) and Landsat 8 (2023) satellite imagery. These images were classified using a supervised classification approach to generate land-use/land-cover maps for each acquisition date. Each land-cover class was then assigned a C factor value based on reference studies conducted in Morocco (Heusch, 1970; Al Karkouri, 2003; Benzougagh, 2020). C factor values range between 0 and 1, where values close to 0 correspond to well-protected areas (e.g., vegetated surfaces or water bodies), and values close to 1 indicate bare soils, which are the most vulnerable to erosion. This spatial variability in the C factor allows the erosion risk estimation to be adjusted according to land-cover types (Fig. 3a, 3b).

Conservation practice factor (P)

The P factor is a dimensionless coefficient representing the effect of soil conservation measures on reducing water erosion at the watershed scale. It reflects the impact of conservation techniques by modifying surface runoff conditions, particularly by decreasing its velocity, intensity, and flow path (Wischmeier& Smith, 1978; Foster & Renard, 1983). Key conservation interventions include gully stabilization, bank protection, and reforestation efforts (Department of Water, Forests, and Soil Conservation, 1995). These practices aim to limit concentrated runoff and reduce the detachment and transport of soil particles. P factor values range from 0 to 1. A value of 1 corresponds to the complete absence of conservation measures, indicating maximum exposure to erosion. Conversely, lower values reflect the presence of effective erosion-control measures capable of significantly reducing soil loss (Fig. 3g, 3h).

RUSLE–GEE model validation

Model validation is a critical step in soil erosion assessment, as it ensures the reliability and applicability of model outputs. In this study, the RUSLE–GEE model was validated using field-measured erosion-related data, providing direct ground-truth information for evaluating satellite-derived estimates. Model outputs were assessed by comparing mean annual soil loss values derived from the GEE-based RUSLE framework with those obtained from ground-based measurements and GIS-based calculations, enabling a robust evaluation of model performance. The use of measured data allowed for a quantitative assessment of the agreement between satellite-driven and field-based erosion estimates, thereby reducing uncertainty commonly associated with remote sensing-based modeling approaches. This validation strategy strengthens the credibility of the RUSLE–GEE application in the Nekor watershed and provides direct evidence of its ability to capture spatial and temporal patterns of soil erosion under varying topographic, lithological, and land-use conditions. The strong consistency observed between measured data, GEE-derived estimates, and values reported in the literature confirms the robustness and reliability of the integrated RUSLE–GEE approach for soil erosion assessment and supports its applicability for watershed-scale erosion monitoring and management.

RESULTS AND DISCUSSION

The assessment of the R factor, which reflects the rainfall-driven erosive intensity, shows considerable spatial variability within the Oued Nekor watershed. In year 2003, R values ranged between 165 and 329,45 $MJ.mm.ha^{-1}.h^{-1}.yr^{-1}$, with an average of 247,22, whereas in year 2023 they varied between 156,07 and 285,61, reaching an average of 242,76 (Table 1 and Figure 4). This spatial pattern highlights a marked heterogeneity, with the most erosion areas located mainly in the central and southern mountainous sectors of the basin. In contrast, areas downstream of the Mohammed Ben Abdelkrim Al Khattabi dam and those in the northern portion of the watershed display the lowest values.

The analysis of rainfall records reveals a marked decline in annual precipitation, dropping from 414,9 mm in year (1983–2003) to 352.21 mm in year (2004–2023), which represents an overall decrease of approximately 8.17%. This downward trend directly affects the R factor, thereby influencing the watershed's erosive potential. Regarding the topographic LS factor, which accounts for both slope length and gradient, values range between 0 and 37.39. According to the spatial distribution map shown in Figure 4e, most of the study area falls within class [0–0.88], representing nearly 82.55% of the total surface. The class associated with the maximum LS value covers about 0.68% of the basin. The morphological configuration of the basin exhibits a markedly pronounced relief in its upstream section (Fig. 5). Approximately 45.85% of the total area lies above 1000 m in elevation. Nearly 32.24% of the basin extends between 500 and 1000 m, while 9.6% is located within the 300-500 m range. Less than 12.32% of the total surface area is situated below 300 m. Hypsometric analysis highlights a gradual increase in elevation from north to south. The surface areas corresponding to each altitudinal interval, along with their respective proportions, were systematically quantified (Table 2). The K factor, which reflects soil susceptibility to erosion, ranges between 0.1 and 0.49. The highest values occur predominantly in highly deformed mountainous regions. These values are mainly linked to marl–clayey soils and mixed soils with

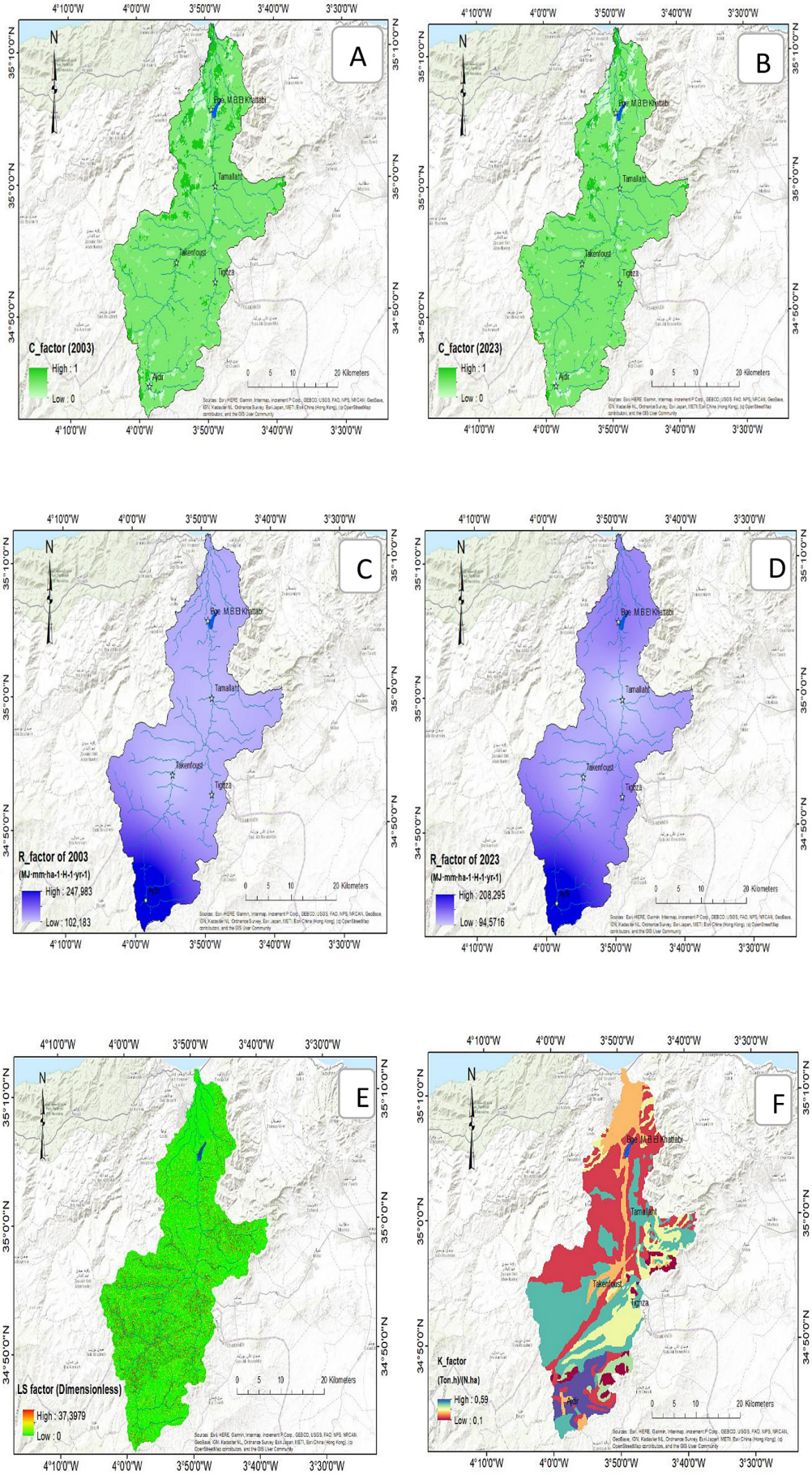
A
C_factor (2003)
High : 1
Low : 0
B
C_factor (2023)
High : 1
Low : 0
C
R_factor of 2003
(MJ·mm·ha-1·H-1·yr-1)
High : 247,983
Low : 102,183
D
R_factor of 2023
(MJ·mm·ha-1·H-1·yr-1)
High : 208,295
Low : 94,5716
E
LS factor (Dimensionless)
High : 37,3979
Low : 0
F
K_factor
(Ton.h)(N.ha)
High : 0.59
Low : 0.1
Tamallaht
Takenfoust
Tighza
Aydi
20 Kilometers

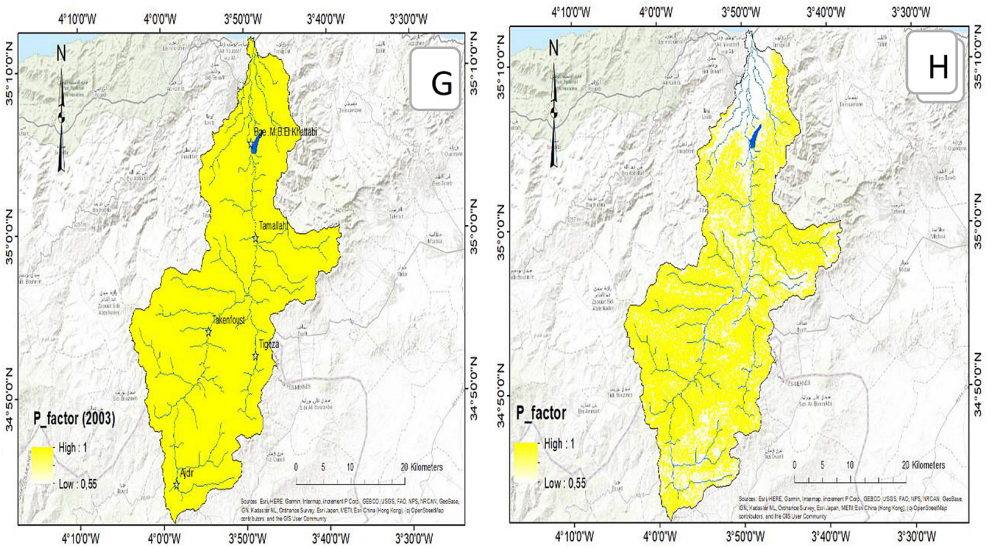

Figure. 3. RUSLE input parameters' spatiotemporal allocation

Table 1. Average precipitation during the period (1983–2003; 2004–2023)

Stations	1983–2003		2004–2023	
	Average precipitation	Converage year	Average precipitation	Converage year
Bge_M.b.A_El_Khattabi	312.875	20	327.225	20
Tamellaht	325.995	20	312.72	20
Takenfoust	297	20	286	20
Tighza	579.06	20	314.35	20
Ajdir	559.615	20	520.75	20
Moyenne	414.904	_	352.209	_

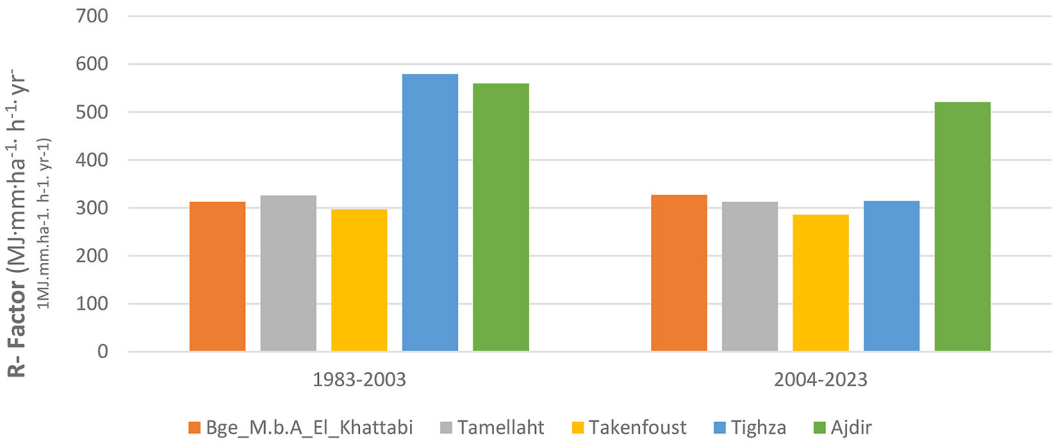

Figure. 4. Evolution of the R-factor over the years

a prevailing clay content, formed on hard geological substrates and commonly associated with dense forest stands, a combination that increases their vulnerability to erosion. These particularly fragile soils are consistent with the classifications previously established by Heusch (1970). The analysis of land use dynamics, based on Landsat 2003 and 2023 imagery, identified the following classes: water bodies, urban areas, bare soils, forests, rangelands, and mixed formations of shrubs and croplands. Due to the spatial resolution of the imagery, urbanization traces are difficult to

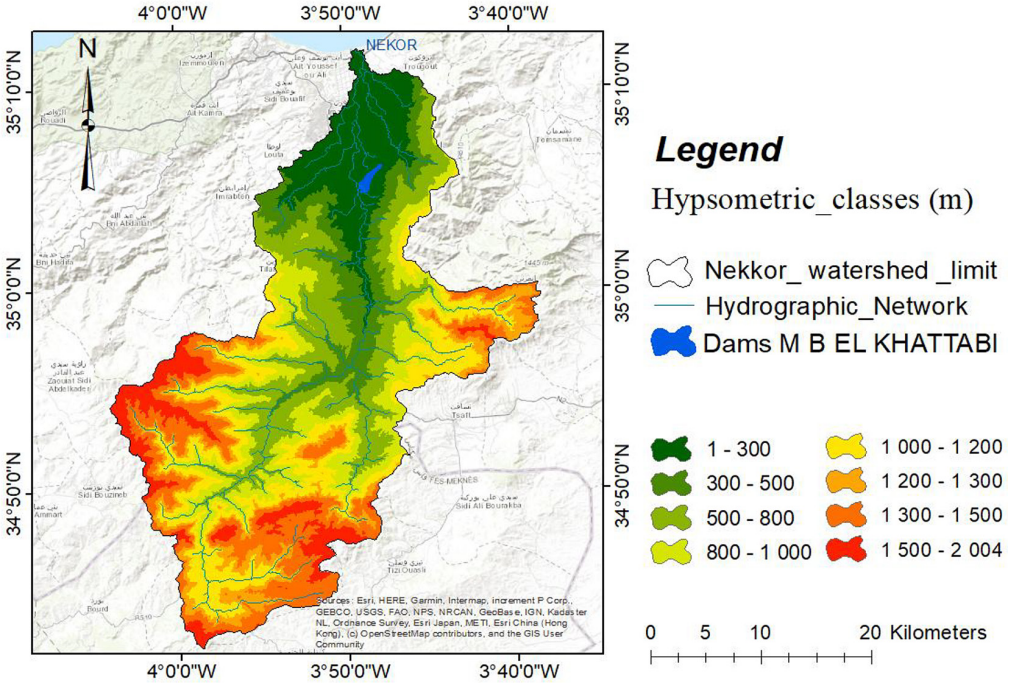

Figure. 5. Map of hypsometric classes

Table 2. Hypsometric classes

Altitudes classes (m)	Surface relative (km²)	Area %
1–300	112.83	12.32
300–500	87.89	9.59
500–800	165.19	18.03
800–1000	130.15	14.21
1000–1200	147.03	16.05
1200–1300	81.18	8.86
1300–1500	130.33	14.23
1500–2004	61.52	6.72
Total	916	100.00

detect, as the watershed remains predominantly rural, sparsely populated, and characterized by dispersed settlements.Over the study period, the extent of bare soils decreased substantially, dropping from 10,7 km^2 to 7,76 km^2, representing a reduction of approximately 2,94 km^2. Likewise, cultivated vegetation experienced a decline, whereas rangelands and urban areas expanded by about 23,82–8,41 km^2 (Table 3).

By integrating all factors of the RUSLE equation (Eq. 1), spatial soil loss maps were produced (Figure 6). The mean annual soil erosion rate exhibited a noticeable decline, decreasing from approximately 47.87 t ha^{-1} yr^{-1} in 2003 to 39.96 t ha^{-1} yr^{-1} in 2023, which corresponds to a reduction of about 7.91 t ha^{-1} yr^{-1}. This decreasing trend is consistent with findings from similar studies conducted in the same region (Okacha et al., 2023).

Similarly, the integration of all RUSLE factors within the Google Earth Engine (GEE) platformenabled the generation of satellite-based soil erosion maps (Figure 7). The GEE-derived mean annual soil erosion rate also shows a clear downward trend, declining from 46.08 t ha^{-1} yr^{-1} in 2003 to 37.04 t ha^{-1} yr^{-1} in 2023, representing a reduction of approximately 9.04 t ha^{-1} yr^{-1}. This trend reflects temporal changes in land cover and soil conservation practices within the watershed and aligns well with erosion dynamics reported in comparable regional studies.

Finally, the classification of areas according to their erosion risk indicates that, in year 2003, approximately 29.76% of the basin area was classified as low-risk, a proportion that increased to 34.14% by year 2023. The results reveal an expansion of nearly 4.38 km^2 for this class, while class [15–30] also expanded by about 1.49 km^2. Conversely, the surface areas corresponding to the higher-risk classes [30–60], [60–90], [90–120] and >120 experienced notable reductions of approximately 0.02 km^2, 1.41 km^2, 0.97 km^2, and 3.47 km^2, respectively (Table 4).

The comparison of soil erosion class percentages between the periods 1983–2003 and

Table 3. List of land use classes

Classes	2003		2023		Evolution
	Area (km²)	Area (%)	Area (km²)	Area (%)	
Water	2.11	0.23	2.63	0.29	0.53
Forset	24.99	2.73	24.16	2.64	-0.83
Floodedvegetation	0.00	0.00	0.10	0.01	0.10
Crops/culture	57.05	6.23	27.34	2.99	-29.71
Urban	42.90	4.69	51.31	5.61	8.41
Bareground	10.70	1.17	7.76	0.85	-2.95
Path/parcours	777.77	84.95	801.59	87.62	23.82
Total	915.51	100	914.89	100	_

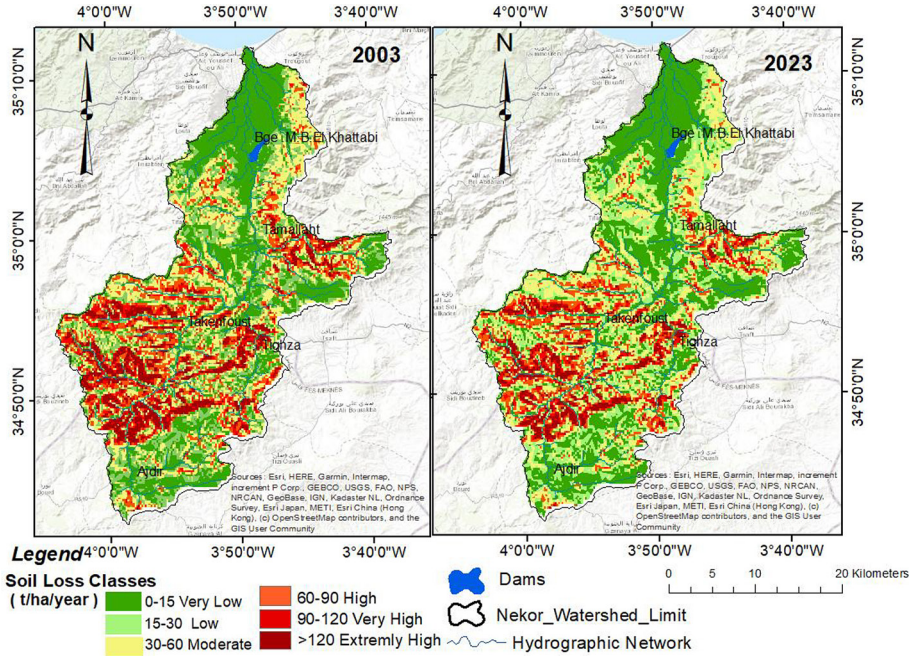

Figure. 6. Maps of spatiotemporal allocation of soil loss rate within Nekor watershed

2004–2023 (Figure 8) reveals a clear shift toward lower erosion intensities across the watershed. During 1983–2003, areas characterized by low erosion rates (0–15 t $ha^{-1}yr^{-1}$) accounted for 31.9% of the total area, increasing to 37.2% in the 2004–2023 period. Similarly, the proportion of the [15–30] t ha^{-1} yr^{-1} class rose slightly from 19.3% to 21.7%. In contrast, moderate to high erosion classes exhibited a general decline over time. The [60–90] t ha^{-1} yr^{-1} class decreased from 11.4% to 9.5%, while the [90–120] t ha^{-1} yr^{-1} and >120 t ha^{-1} yr^{-1} classes dropped from 5.7% and 8.4% to 4.3% and 5.2%, respectively. Overall, these changes indicate a reduction in severe erosion-prone areas, likely reflecting improvements in land cover conditions and the implementation of soil conservation practices over the last two decades.

These findings indicate that the implementation of soil conservation measures has played a significant role in reducing soil loss, particularly in the most erosion prone areas of the watershed. Moreover, the observed trends align with the conclusions of previous research, which demonstrated the effectiveness of conservation practices such as terracing, vegetation restoration, and contour farming in mitigating erosion (Li et al., 2011; Fowler et al., 2022; Wu et al., 2022). However, it is important to emphasize that these improvements are not solely the result of land management interventions, as external environmental factors, particularly climatic variability, exert a strong influence on erosion dynamics. Interestingly, although total precipitation decreased between the two study periods, this decline did not lead to a proportional reduction in

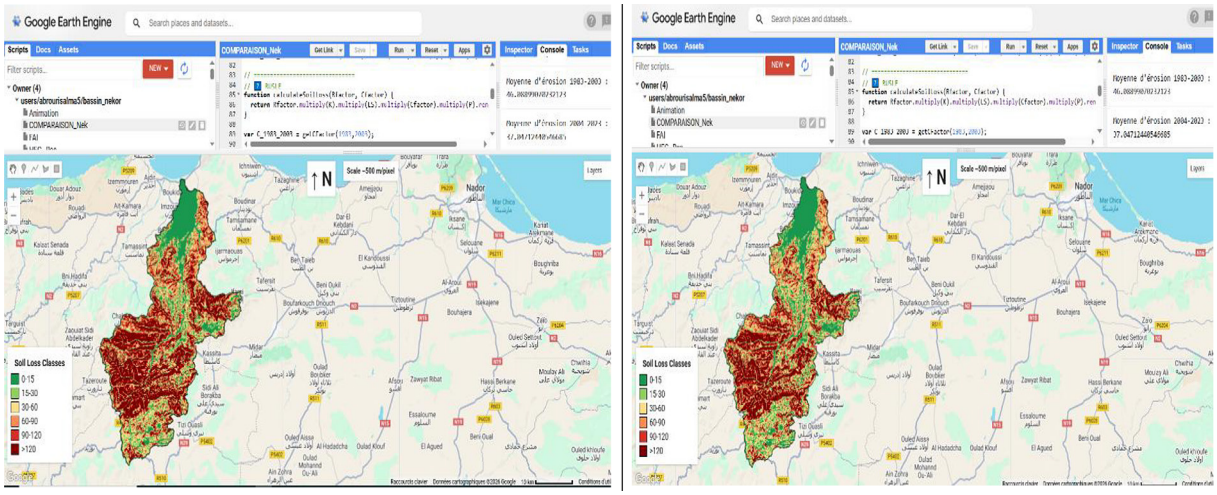

Figure. 7. Maps of spatiotemporal allocation of soil loss rate within Nekor watershed

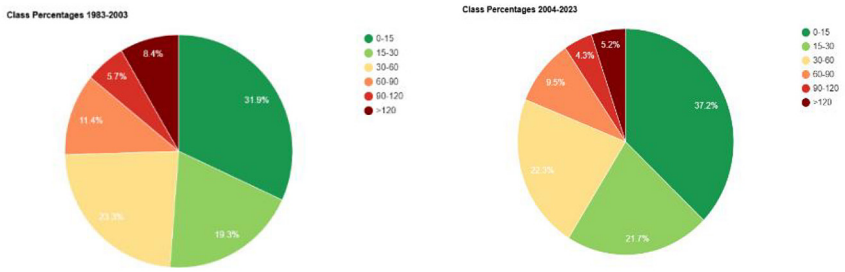

Figure. 8. Temporal variation in soil erosion class distribution for the periods 1983–2003 and 2004–2023**.**

Table 4. Evolution of risk classes and erosion rates (1983–2003; 2004–2023)

Risk	Classes (t/ha/year)	2003		2023		Evoltution (km²)
		Area (km²)	Area (%)	Area (km²)	Area (%)	
Very low	15	267.95	29.76	307.18	34.14	4.38
Low	30	163.23	18.13	176.52	19.62	1.49
Moderate	60	216.18	24.01	215.91	23.99	- 0.02
High	90	107.59	11.95	94.83	10.54	-1.41
Very high	120	58.70	6.52	49.94	5.55	-0.97
Extremly high	>120	86.70	9.63	55.44	6.16	-3.47
Erosion rate (t/ha/year)	Total	463.1		389.02		-74.08
	Moyen	47.87		39.96		-7.91

erosion rates. This inconsistency can be explained by a more uniform temporal distribution of rainfall events, which tends to reduce the occurrence of intense runoff and enhance water infiltration, thereby lowering soil detachment and transport (Pruski& Nearing, 2002). Therefore, to better understand the complexity of these interactions, a more detailed climatic assessment is warranted. Such an analysis should integrate rainfall intensity, duration, and frequency indices, in order to evaluate how changing precipitation patterns rather than total amounts shape erosion responses within the Nekor watershed. Overall, incorporating these factors would provide a clearer and more comprehensive picture of how conservation strategies and evolving climate conditions jointly influence long term soil stability.

Correlation between GIS- and GEE-derived area estimates

The comparison between areas estimated using GIS and those derived from Google Earth

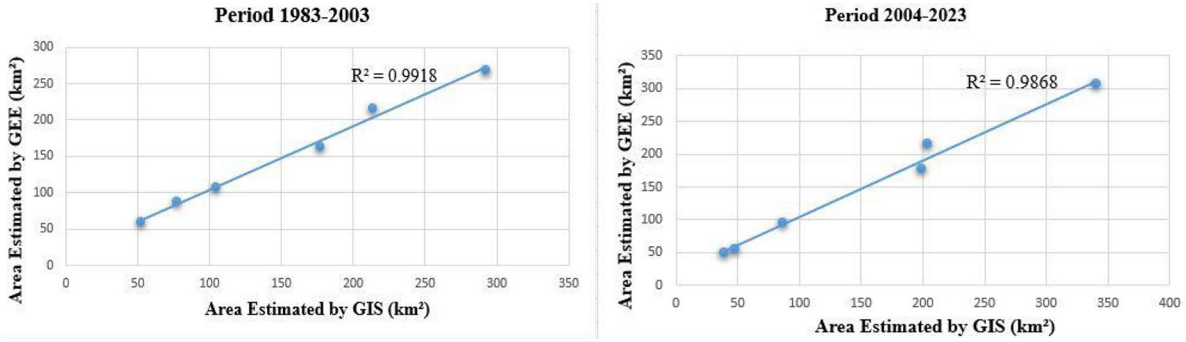

Figure.9. Correlation between GIS and GEE area estimates for two study periods

Engine (GEE) reveals a very strong linear relationship for both analyzed periods (Figure 9). During the period 1983–2003, the regression analysis shows an excellent agreement between the two methods, with a coefficient of determination of $R^2 = 0.9918$, indicating that GEE-based estimates closely match the GIS-derived reference areas. Similarly, for the period 2004–2023, a high correlation is observed ($R^2 = 0.9868$), confirming the robustness and consistency of GEE in capturing spatial variations in the estimated areas over time. Although a slight increase in dispersion is noticeable in the recent period, the overall results demonstrate that GEE provides reliable area estimates comparable to traditional GIS approaches. These findings highlight the effectiveness of GEE as a rapid and accurate tool for large-scale spatial analysis, particularly for long-term environmental monitoring where conventional GIS processing may be more time-consuming.

CONCLUSIONS

Water erosion remains a major driver of soil degradation in mountainous Mediterranean environments, with serious implications for ecosystem functioning, agricultural productivity, and water resource sustainability. In the Nekor watershed, this process directly contributes to accelerated sedimentation in the Mohamed Ben Abdelkrim El Khattabi Dam, progressively reducing reservoir storage capacity and threatening long-term water security in the Rif region. The results of this study confirm that marl-schist and calcareous formations are particularly susceptible to erosion due to their weak structure, fine texture, steep slopes, and limited vegetation cover, making them critical sources of sediment under intense runoff conditions.

By combining field-based measurements, conventional GIS analysis, and satellite-derived data processed within Google Earth Engine, this research provides a robust assessment of soil erosion dynamics over a 40-year period (1983–2023). The close agreement between GEE-based RUSLE estimates and ground-based GIS results demonstrates the reliability and accuracy of satellite-derived datasets for long-term soil erosion assessment. Both approaches reveal a comparable reduction in mean annual soil loss since the early 2000s, reflecting the positive impact of soil and water conservation measures implemented within the watershed.

The spatiotemporal analysis highlights that erosion hotspots are primarily concentrated in upstream areas characterized by steep terrain, fragile lithology, and sparse vegetation cover. These zones remain priority targets for future soil conservation and sediment control interventions. The observed decline in erosion rates underscores the effectiveness of conservation practices; however, persistent vulnerability in certain sub-basins indicates the need for sustained and adaptive management strategies.

Beyond erosion quantification, this study demonstrates the added value of integrating RUSLE within a cloud-based GEE environment. This approach significantly reduces computational constraints, enables rapid and repeatable analyses, and facilitates access to long-term, multi-source geospatial datasets. As such, it offers a cost-effective, scalable, and transferable framework for soil erosion monitoring, particularly in data-scarce regions.

Effective mitigation of soil erosion and reservoir sedimentation in the Nekor watershed requires an integrated watershed-scale strategy that accounts for geological conditions, climatic variability, vegetation dynamics, topography, and

land-use practices. Priority actions should include targeted conservation measures in erosion-prone upstream areas, restoration of degraded lands, promotion of sustainable agricultural practices adapted to local pedoclimatic conditions, and continued engagement of local communities through awareness, training, and capacity-building initiatives. The validated GEE–RUSLE framework developed in this study provides decision-makers with a reliable tool to support evidence-based planning and the long-term sustainability of soil and water resources in the Rif Mountains.

REFERENCES

1. ABHL (Agence du Bassin Hydraulique du Loukkos). 2015. *Plan directeur d'aménagement intégré des ressources en eau du bassin de la Loukkos.* Rapport technique. Agence du Bassin Hydraulique du Loukkos, Maroc.
2. Al Karkouri, J. 2003. *Évaluation de l'érosion hydrique par la méthode RUSLE dans le bassin versant de l'Oued Beht (Moyen Atlas, Maroc).* Mémoire de D.E.S.A., Université Mohammed V, Rabat.
3. Arnoldus, H.M.J. 1977. *Methodology Used to Determine the Maximum Potential Average Annual Soil Loss Due to Sheet and Rill Erosion in Morocco*. FAO Soils Bulletin 34.
4. Arnoldus, H.M.J. 1980. An Approximation of the Rainfall Factor in the Universal Soil Loss Equation. Dans *Assessment of Erosion,* édité par M. de Boodt et D. Gabriels. Wiley.
5. Arrebei, F., Cheggour, A., Barakat A., Aabdellaoui, A. 2019. Assessment of Sediment Yield in the Nekor Watershed Using RUSLE Model. *Revue Marocaine de Géomorphologie*.
6. Arrebei, N., Sabir, M., Naimi, M., Chikhaoui, M., Raclot, D. 2020. Assessment of Soil Erosion with RUSLE 3D and USPED in the Nekor Watershed (Northern Morocco). *Open Journal of Soil Science,* 10(12), 631–42. https://doi.org/10.4236/ojss.2020.1012031.
7. Benzougagh, Y. 2020. *Analyse spatiale de l'érosion hydrique dans le bassin versant de l'oued Nekor (Rif, Maroc) à l'aide du modèle RUSLE et de la télédétection*. Mémoire de Master, Université Abdelmalek Essaâdi.
8. Benmansour, M., Er-Raki, S., Khabba, S. 2020. Soil erosion in the semi-arid and arid regions of Morocco: Current status and future perspectives. *Sustainability*, *12*(6), 2345.
9. Chalouan, A., Michard, A., Feinberg, H., Montigny, R., Saddiqi, O. 2008. The rif mountain building (Morocco): A new tectonic scenario. *Géologie Alpine,* 85, 1–70.
10. Chanyour, Y., El Achari O. 2022. Bilan des études géographiques sur l'érosion hydrique dans les montagnes du Rif (Maroc). *Études Géographiques*, 2022(1), 45–62.
11. Département des Eaux, Forêts et de la Conservation des Sols. 1995. *Stratégie nationale de conservation des sols et de lutte contre l'érosion hydrique au Maroc*. Rabat : Ministère de l'Agriculture et de la Mise en Valeur Agricole.
12. Dumas, J. 1965. Relation entre l'érodibilité des sols et leurs caractéristiques analytiques. *Cahiers ORSTOM: série Pédologie*, 3(4), 307–333
13. Dumas, J. 1978. *Le Rif central: étude géomorphologique*. Bordeaux: Publications de l'Université de Bordeaux.
14. El Abbassi, H. 1997. Quelques aspects des transformations récentes dans les campagnes du Rif oriental marocain: mécanismes, formes et incidences sur le milieu. *Annales de géographie*, 597, 479–501.
15. El Hammoudani, Y., Dimane F. 2021. Occurrence and fate of micropollutants during sludge treatment: Case of Al-Hocéima WWTP, Morocco. *Environmental challenges, 5*, 100321.https://doi.org/10.1016/j.envc.2021.100321
16. Elnashar, A., Zeng, H., Wu, B., Fenta, A.A., Nabil, M., Duerler, R. (2021). Soil erosion assessment in the Blue Nile Basin driven by a novel RUSLE-GEE framework. Science of the Total Environment, *793*, 148466.
17. Fentaw, A.E., Abegaz, A. (2024). Soil erosion assessment and identification of erosion hotspot areas in the upper Tekeze Basin, Northern Ethiopia. Heliyon, *10*(12).
18. FAO. 2006. *Status of the World's Soil Resources*. Rome: FAO.
19. FAO. 2015. *Status of the World's Soil Resources*. Rome: FAO.
20. Foster, G.R., Renard, K.G. 1983. Soil conservation: principles of erosion by water. *Dans dryland agriculture,* (Eds.) H.E. Dregne et W. O. Willis, 155–76. Laouina Madison, WI: American Society of Agronomy.
21. Fowler, Keirnan, J.A., Murray Peel, C., Margarita Saft, R.J., Nathan, Avril Horne, R.L. Wilby, Connor McCutcheon, Peterson T.J. 2022. Hydrological shifts threaten water resources. *Water Resources Research,* 58(8), e2021WR031210. https://doi.org/10.1029/2021WR031210
22. Jodhani, K.H., Patel, D., Madhavan, N., Singh, S. K. (2023). Soil erosion assessment by rusle, google earth engine, and geospatial techniques over rel river watershed, gujarat, india. *Water Conservation Science and Engineering*, *8*(1), 49.
23. Gao, Jiangbo, et Huan Wang. 2018. Spatial gradient and quantitative attribution of karst soil erosion in Southwest China. *Environmental Monitoring*

and Assessment, 190, 730. https://doi.org/10.1007/s10661-018-7116-2

24. García-Orenes, F., Roldán, A., Mataix-Solera, J., Cerdà, A., Campoy, M., Arcenegui, V., Caravaca, F. 2009. Soil structural stability and erosion rates influenced by agricultural management practices in a semi-arid mediterranean agro-ecosystem. *Soil Use and Management*, *25*(3), 297–305. https://doi.org/10.1111/j.1475-2743.2009.00233.x
25. García-Orenes, F., A. Cerdà, J. Mataix-Solera, C. Guerrero, M.B., Bodí, V. Arcenegui, R. Zornoza, Sempere J.G. 2010. Effects of agricultural management on surface soil properties and organic carbon in a mediterranean agro-ecosystem. *Soil and Tillage Research, 107*(2), 324–30. https://doi.org/10.1016/j.still.2010.01.007.
26. HCEFLCD (Haut-Commissariat aux Eaux et Forêts et à la Lutte contre la Désertification). 2014. *Étude de la vulnérabilité des sols à l'érosion dans les massifs du Rif*. Publication du Haut-Commissariat aux Eaux et Forêts, Maroc.
27. Heusch, B. 1970. *Le Rif marocain: étude géographique*. Paris : Presses Universitaires de France.
28. Heusch, B. 1970. *L'érosion en Afrique du Nord : aspects, causes et mesures de lutte antiérosive*. Paris : ORSTOM.
29. Iouzzi, N., Larabi A., Faouzi M. 2011. Modélisation hydrodynamique de la nappe de RhisNekor (Maroc) et impact de l'intrusion marine. Dans *Coastal and Maritime Mediterranean Conference*, 2[e]éd., Tanger, Maroc. https://doi.org/10.5150/cmcm.2011.072.345.
30. Laouina, A. 1995. Le Maroc nord oriental : reliefs, modelés et dynamique du calcaire. Rabat: Université Mohammed V.
31. Lal, R. 2001. Soil degradation by erosion. *Land Degradation & Development*, 12(6), 519–39. https://doi.org/10.1002/ldr.472.
32. Li, Xiaoming, Yujie Zhang, Hua Wang, et al. 2011. Impact of soil erosion on crop yield in Eastern China. *Agricultural Sciences, 23*(4), 245–56.
33. Maaliou, A., Faouzi M., Sadiki A. 2014. Estimation de l'érosion hydrique dans le bassin versant de l'oued Beht (Maroc) par l'application du modèle RUSLE. *European Scientific Journal, 10*(24), 264–82.
34. Manrique, L.A. 1988. *Land erodibility assessment methodology: LEAM, using soil survey data based on soil taxonomy.* 1st ed., November 1988. Editorial & Publication Shop.
35. Moore, Ian D., Burch J.G. 1986. Physical basis of the length slope factor in the universal soil loss equation. *Soil Science Society of America Journal, 50*(5), 1294–98. https://doi.org/10.2136/sssaj1986.03615995005000050042x
36. Morgan, R.P.C. 2005. Soil Erosion and Conservation. 3e éd. Blackwell Publishing.
37. Niazi, M., Khalil A., Messaoudi M. 2005. L'érosion dans le Rif oriental : état des lieux. *Géomorphologie: Relief, Processus, Environnement*, 11(2), 123–34.
38. Niazi, S., Snoussi M., et Foutlane A. 2005. Impact des aléas climatiques sur la qualité des eaux d'un hydrosystème aménagé en zone semi-aride: cas du bassin versant du Nekor (Maroc). *Sécheresse*, 16(3), 183–87.
39. Observatoire du Sahara et du Sahel (OSS). 2020. *État des lieux du secteur de l'eau au Maroc.* Projet CREM. https://projet.oss-online.org/maghreb-eau/sites/default/files/2020-01/Etat-des-Lieux-Secteur-Eau-Maroc.pdf.
40. Okacha, A. 2020. *Pressions anthropiques et dégradation des milieux naturels dans le Rif oriental.* Mémoire de Master, Université Abdelmalek Essaâdi, Faculté des sciences Rabat-Tétouan.
41. Okacha, A., Salhi A., Arari K., El Badaoui K., Lahrichi K. 2023. Soil erosion assessment using the RUSLE model for better planning: A case study from Morocco. *Modeling Earth Systems and Environment*, 9, 3731. https://doi.org/10.1007/s40808-023-01731-4
42. Papaiordanidis, S., Gitas, I.Z., Katagis, T. (2019). Soil erosion prediction using the revised universal soil loss equation (RUSLE) in Google Earth Engine (GEE) cloud-based platform., 100, 36-52.
43. Pruski, F.F., Nearing J.A. 2002. Climate-induced changes in soil erosion in the United States. *Journal of Soil and Water Conservation*, 57(1), 7–16.
44. Renard, K.G., Foster, G.R., Weesies, G.A., McCool, D.K., Yoder D.C. 1997. *Predicting Soil Erosion by Water: A Guide to Conservation Planning with the Revised Universal Soil Loss Equation (RUSLE*). USDA Agriculture Handbook No. 703.
45. Salhi, A. 2008. *Étude géodynamique et sismotectonique de la région du Rif (Maroc).* Thèse de doctorat, Université Mohammed V, Rabat.
46. Salhi, A., Benssaou M., El Ayadi H. 2019. Impact of land use changes on hydrological response and erosion risk in the Nekor Watershed. *Revue des Sciences de l'Eau.*
47. Salhi, A., et al. 2022. Climatic variability and its implications on water resources in the Rif Region. *Hydrology and Earth System Sciences*.
48. Wischmeier, W.H., Smith D.D. 1978. *Predicting rainfall erosion losses: a guide to conservation planning.* USDA Agriculture Handbook, 537. Washington, D.C.: U.S. Government Printing Office.
49. Wu, L., Chen K., Zhao P., et al. 2022. Advances in erosion modeling using remote sensing data. *Journal of Environmental Management, 310*, 114754.